

¹ **Submesoscale streamers exchange water on the north
2 wall of the Gulf Stream**

³ Jody M. Klymak¹, R. Kipp Shearman², Jonathan Gula³, Craig M. Lee⁴, Eric A. D'Asaro⁴, Leif N.
⁴ Thomas⁵, Ramsey Harcourt⁴, Andrey Shcherbina⁴, Miles A. Sundermeyer⁶, Jeroen Molemaker⁷
⁵ & James C. McWilliams⁷

⁶ ¹*University of Victoria, Victoria, British Columbia, Canada*

⁷ ²*Oregon State University, Corvallis, Oregon, USA*

⁸ ³*Laboratoire de Physique des Océans, Université de Bretagne Occidentale, Brest, France*

⁹ ⁴*Applied Physics Laboratory, University of Washington, Seattle, Washington USA*

¹⁰ ⁵*Stanford University, Stanford, California, USA*

¹¹ ⁶*University of Massachusetts Dartmouth, Dartmouth, Massachusetts, USA*

¹² ⁷*University of California, Los Angeles, California, USA*

¹³ **The Gulf Stream is a major conduit of warm surface water from the tropics to the subpolar**
¹⁴ **North Atlantic. Its north side has a strong temperature and salinity front that is less than 5**
¹⁵ **km wide that is maintained for hundreds of kilometers despite considerable energy available**
¹⁶ **for mixing. Large mesoscale (> 20 km) “rings” often pinch off, but like the Gulf Stream they**
¹⁷ **are resistant to lateral mixing, and retain their properties for a long time. Here we observe**
¹⁸ **and simulate a sub-mesoscale (< 20 km) mechanism by which the Gulf Stream exchanges**
¹⁹ **water with the cold subpolar water to the north. The front exhibits a strong temperature-**
²⁰ **salinity contrast, with a distinct mode of “mixed” water between the two water masses. This**

21 **mass of water is not seen to increase downstream despite there being substantial energy avail-**
22 **able for mixing. A series of “streamers” detrain some of this water from the Gulf Stream at**
23 **the crest of meanders. Subpolar water is entrained replacing the mixed water, and helping**
24 **to resharpen the front. The water mass exchange can account for a northwards flux of salt**
25 **of $0.8 - 5 \text{ psu m}^2\text{s}^{-1}$, which can be cast as an effective local diffusivity of $O(100 \text{ m}^2\text{s}^{-1})$. This**
26 **is similar to bulk-scale flux estimates of $1.2 \text{ psu m}^2\text{s}^{-1}$ and is enough to supply fresh water to**
27 **the Gulf Stream as required for the production of 18-degree subtropical mode water.**

28 The Gulf Stream (GS) is the western boundary current of the North Atlantic subtropical
29 wind-driven circulation. It separates from Cape Hatteras and extends into the interior North At-
30 lantic, traveling east. As it does so, it loses heat not only to the atmosphere, but also by mixing
31 with the cold water in the subpolar gyre to the north. It also becomes fresher, an observation that
32 can only be explained by entrainment of fresh water from the north¹. As it entrains water, the GS
33 increases its eastward transport by approximately $4 - 8 \times 10^6 \text{ m}^3\text{s}^{-1}/100 \text{ km}$ (Johns et. al.²).

34 The GS has a sharp density front, but it also has a sharp temperature and salinity front, as has
35 been demonstrated at the surface from shipboard surveys³ and satellite images⁴. The sharpness of
36 the front beneath the surface has been less-clear, and requires high-resolution lateral sampling to
37 resolve. It is also known that the front has a sharp potential vorticity gradient⁵, and such gradients
38 act as a barrier to lateral mixing^{6,7}. Despite this barrier, property budgets indicate that there is
39 significant exchange across the north wall¹, and that entrainment of fresh water is necessary to
40 create the dynamically important “18-degree water” that fills much of the upper Sargasso Sea.

41 The mechanisms controlling this lateral mixing have not been identified. There are large
42 eddies that periodically pinch off the GS and carry warm water to the north. However, some of
43 these are re-entrained into the GS and do not result in a net exchange. Instead, tracer budgets
44 across the front appear to be dominated by small-scale processes⁸. To date some of the best direct
45 evidence for cross-front exchange consists of the trajectories of density-following floats placed
46 at the north wall^{9,10}. These floats were observed to regularly detrain from the GS, such that of
47 95 floats, 26 stayed in the GS, 7 were detrained in rings, and 62 were detrained by mechanisms
48 other than rings¹⁰. Kinematic theories have been examined to explain the detrainment of the floats
49 ¹¹⁻¹³, and the similarity of the float detrainment to satellite images of “streamers” of warm water
50 detraining from the Gulf Stream have been noted. However, direct observations of the processes
51 as it occurs at depth have been lacking.

52 Here we present evidence that there is small-scale mixing (<0.5 km) on the northern cy-
53 clonic side of the GS, and that the mixed water periodically peels off the GS in thin (5-10 km
54 wide) “streamers”. In March 2012 we made high-resolution measurements of the north wall of
55 the GS from 66 W to 60 W (Fig. 1), about 850 km east of where the GS separates from the North
56 American continental slope. Two research vessels tracked a water-following float placed in the GS
57 front and programmed to follow the density of the surface mixed layer. The float was transported
58 downstream with a speed of $1.4 \pm 0.2 \text{ m s}^{-1}$, in water that became denser as the surface of the GS
59 cooled. One vessel maintained tight sampling around the float and deployed an undulating profiler
60 to 200 m, making 10-km cross sections every 10 km downstream. The second vessel had an undu-
61 lating profiler making larger 30-km scale sections. Both profilers measured temperature, salinity

62 and pressure, and had approximately 1-km along-track resolution; both ships also measured ocean
63 currents. Fluorescent dye was deployed near the floats on some deployments, and measured by the
64 profilers on the ships. By following the float, a focus on the front was maintained as it curved and
65 meandered to the east.

66 During these observations, the GS had a shallow meander crest at 65 W (Fig. 1b) followed
67 by a long concave region (63 W) and then another large crest (61 W). Satellite measurements show
68 the sharp temperature changes across the front, superimposed with thin intermediate-temperature
69 ($15\text{-}18^{\circ}\text{C}$) streamers detaining to the north at approximately 65 W, 64 W, and at the crest of
70 the large meander at 61 W. An older streamer that has rolled up can also be seen at 62 W. The
71 ships passed through the three newer streamers providing the first detailed observations of their
72 underwater structure.

73 The front consists of density surfaces that slope up towards the north (Fig. 2a-d). The water
74 along density surfaces is saltier (and warmer) in the GS, and fresher (and colder) to the north.
75 The transition between the two water masses is remarkably abrupt, occurring over less than 5-km.
76 This sharpness persisted from our western-most section during the cruise (71.5 W) to the eastern-
77 most (60.5 W). Some cross sections clearly show lateral interleaving of salinity north of the front
78 (Fig. 2a) with approximately 5-km wide salinity anomalies ($S \approx 36.15$ psu). These anomalies
79 move slower than the front (Fig. 2e), and have high potential vorticity that is normally associated
80 with the front (Fig. 2i).

81 The temperature-salinity (T/S) relationship of this data shows the contrast between the GS

82 and the subpolar water as two distinct modes (Fig. 3a), except near the surface where the water
83 masses are strongly affected by the atmosphere. For the deeper water, there is a third distinct
84 population between the two larger modes in T/S space that represents the water in the salinity
85 anomalies, and we have labelled as “streamers”. The distinctness in T/S space of the streamers
86 indicates that after the GS and subpolar waters mixed, the partially mixed water continued to mix,
87 condensing it in T/S space (perfectly mixed water would be a dot).

88 Looking at the GS in plan view (Fig. 3b) we see the mixed water that makes up the
89 streamers is connected along the length of our observations. The first streamer (64.5 W) is hor-
90 izontally connected over 100 km, and is about 5 km wide, and at least 150 m deep. Where the
91 streamer is the most detached (Fig. 2a) the main front is the sharpest of the 4 cross sections.
92 Downstream of this streamer, the mixed water thins before the eastern meander (60.5 W) where
93 there is a second streamer. Further downstream, the mixed water almost disappears by the last
94 cross-section (59 W). There is a hint of a streamer north of the front here, but our section did not
95 go far enough north to define it, but the thinning of the front is strong evidence that water has been
96 removed in a streamer.

97 We can quantify the rate of detrainment from the first streamer (64.5 W). It starts on the
98 fast side of the front with water flowing approximately 0.25 m s^{-1} faster than the float (Fig. 2h).
99 Upstream, where it is detached (Fig. 2e), it is flowing almost 0.5 m s^{-1} slower than the float. A
100 5-km wide and 150-m deep streamer, with a relative velocity of 0.75 m s^{-1} represents a rate of
101 detrainment of over $0.5 \times 10^6 \text{ m}^3 \text{s}^{-1}$.

102 Concurrently, there is a bolus of fresh water from the north that is enfolded between the
103 streamers and the GS, which we will call an “intrusion”. The entrainment of the intrusion is hard
104 to quantify using the data presented above, because it is drawn from a large pool of water upstream.
105 However, a subsequent survey of the north wall (March 14) included a dye release in this water
106 that was then entrained in an intrusion (Fig. 4a-c). The streamer during this occupation was less
107 pronounced than the one described above, but was clear for a number of passes through the north
108 wall. The dye cloud was quite spread out, but the data show clear interleaving of the intrusion
109 water.

110 High-resolution numerical simulations ($dx \approx 500m$, see Methods) resolve these features
111 and also confirm the entrainment of the fresh intrusion (Fig. 4d-i). Seeding the simulation with La-
112 grangian particles (see methods) allows us to track the evolution of the streamers and the intrusion
113 as the flow moves downstream. Before the streamer is formed, the water in the intrusion (ma-
114 genta contours) is near the surface and the streamer water (green contours) is well within the front
115 (Fig. 4d,g). Downstream (Fig. 4e,h) the fresh water has been subducted to 150 m depth, and the
116 streamer has been pushed north of the front. Both water masses accelerate with the GS (Fig. 4f),
117 but the fresh intrusion accelerates more, such that the intrusion is entrained and the streamer slows
118 and is detrained. As in the observations, the streamer occupies an intermediate region in T-S space
119 (Fig. 4i, green contour), and originates in the high-vorticity region of the front. The acceleration
120 of the fresh intrusion relative to the streamer is an important finding of the model, as the fresh
121 water now forms a new sharp T-S front with the warm salty GS, and the mixed streamer water is
122 carried away from the front. The model further shows that the streamers are more prominent on

¹²³ the leading edges of meanders, also clearly seen in satellite images (Fig. 1).

¹²⁴ There are two major implications of the loss of mixed water to the north. The first is that
¹²⁵ it helps explain why the front at the north wall of the GS remains so sharp. The T/S distribution
¹²⁶ clearly indicate that there is mixing because of the separate water-class mode. However we also
¹²⁷ show that the mixing product is carried away in the streamers. It is striking that it is only the mixed
¹²⁸ water that is carried away, and not high-salinity GS water (Fig. 3b) and that this is also high-
¹²⁹ vorticity water. This implies a dynamical link that we have not seen explored. Streamers have
¹³⁰ been observed in surface temperature satellite images and indirectly by subsurface floats^{9,11,14,15},
¹³¹ and this has led to kinematic models in which particles are displaced from streamlines going around
¹³² propagating meanders^{13,14,16}. The observations here add to these models by showing that it is only
¹³³ mixed water that leaves the GS. This co-incidence indicates to us a role for small-scale mixing
¹³⁴ in producing the destabilizing forces that cause this water to detrain from the north wall. The
¹³⁵ observations and simulation indicate that the meanders of the GS play an important role in the
¹³⁶ formation of the streamers.

¹³⁷ The second implication is that the streamers are a mechanism that can balance large-scale
¹³⁸ budgets that require significant exchange across the GS^{1,8}. Such budgets suggest that this region
¹³⁹ of the GS loses salinity to the north at a rate of $1.2 \text{ psu m}^2 \text{s}^{-1}$ ¹. Each streamer transports $0.2 -$
¹⁴⁰ $0.5 \times 10^6 \text{ m}^3 \text{s}^{-1}$ of water that is $0.8 - 1 \text{ psu}$ saltier than the water that is entrained. Streamers
¹⁴¹ appear approximately every 100-300 km, associated with meanders, so an estimate of their average
¹⁴² transport is $0.8 - 5 \text{ psu m}^2 \text{s}^{-1}$, bracketing the large-scale estimates. Working against a gradient

¹⁴³ of 1 psu/10 km over 200 m depth, the equivalent lateral diffusivity is $40 - 250 \text{ m}^2\text{s}^{-1}$. More
¹⁴⁴ observations would need to be made to make this transport estimate more robust.

¹⁴⁵ Here we have observed a submesoscale lateral stirring process along the north wall of the
¹⁴⁶ GS. The T/S front remains persistently sharp, despite small-scale mixing evident from the T/S dia-
¹⁴⁷ grams, and due to a number of possible processes^{17,18}. The mixed water mass does not accumulate,
¹⁴⁸ or it would weaken the sharpness of the front. Here we show that the streamers detrain the mixed
¹⁴⁹ water, and entrain cold and fresh water toward the north wall, resharpening the temperature-salinity
¹⁵⁰ front. Further analysis of the data and models will shed light on the exact mechanism triggering
¹⁵¹ the ejection of water from the front via the streamers.

¹⁵² 1 Methods

¹⁵³ The Lagrangian float was placed in the Gulf Stream front based on a brief cross-stream survey,
¹⁵⁴ and programmed to match the density of the surface mixed layer (upper 30 m). The float moved
¹⁵⁵ downstream at a mean speed of 1.4 m s^{-1} . The *R/V Knorr* tracked the float and deployed a Chelsea
¹⁵⁶ Instruments TriAxis that collected temperature, salinity, and pressure (CTD) on a 200-m deep
¹⁵⁷ sawtooth with approximately 1-km lateral spacing in a 10-km box-shaped pattern relative to the
¹⁵⁸ float (Fig. 1, magenta). *R/V Atlantis* maintained a larger set of cross sections approximately 30 km
¹⁵⁹ across the front, trying to intercept the float on each front crossing. *R/V Atlantis* was deploying a
¹⁶⁰ Rolls Royce Marine Moving Vessel Profiler equipped with a CTD that profiled to 200 m approx-
¹⁶¹ imately every 1 km. Both ships had a 300 kHz RDI Acoustic Doppler Current Profiler (ADCP)

¹⁶² collecting currents on 2-m vertical scale averaged every 5 minutes (approximately 1 km lateral
¹⁶³ scale), collected and processed using UHDAS and CODAS (<http://currents.soest.hawaii.edu>¹⁹).
¹⁶⁴ This data reached about 130 m, and was supplemented at deeper depths with data from 75 kHz
¹⁶⁵ RDI ADCPs, with 8-m vertical resolution.

¹⁶⁶ Data were interpolated onto depth surfaces by creating a two-dimensional interpolation onto
¹⁶⁷ a grid via Delauney triangulation. No extrapolation was performed. Data on the 26.25 kg m^{-3}
¹⁶⁸ isopycnal were assembled at each grid point by finding the first occurrence of that isopycnal in
¹⁶⁹ depth.

¹⁷⁰ Potential vorticity is calculated from the three-dimensional grid as

$$q = -\frac{g}{\rho_0} (\nabla \times \mathbf{u} + \mathbf{f}) \cdot \nabla \rho, \quad (1)$$

¹⁷¹ where f is the Coriolis frequency, g the gravitational acceleration. The bracketed term is twice
¹⁷² the angular velocity, including the planet's rotation, and the gradient of density represents the
¹⁷³ stretching or compression of the water column. In the GS, the potential vorticity is dominated by
¹⁷⁴ contributions from the vertical density gradient and the cross-stream gradient of the along-stream
¹⁷⁵ velocity:

$$q \approx N^2 \left(-\frac{\partial u}{\partial y} + f \right). \quad (2)$$

¹⁷⁶ Dye Release. At select times during the float evolutions, fluorescein dye releases (100 kg
¹⁷⁷ per release) were conducted at depth as close as possible to the float. Dye was pumped down a
¹⁷⁸ garden hose to a tow package deployed off the side of the ship, consisting of a CTD and a dye

179 diffuser. Prior to injection, the dye was mixed with alcohol and ambient sea water to bring it to
180 within 0.001 kgm^{-3} of the float's target density. Initial dimensions of the dye streak were ≈ 1
181 km along-stream, $\approx 100 \text{ m}$ cross-stream (after wake adjustment), and ranging from 1 - 5 m in the
182 vertical. The TriAxis system on the *R/V Knorr* tracked the fluorescein from its CTD package.

183 Numerical simulation. The high-resolution realistic simulation of the GS is performed with
184 the Regional Oceanic Modeling System (ROMS²⁰). This simulation has a horizontal resolution of
185 500m and 50 vertical levels. The model domain spans 1,000 km by 800 km and covers a region
186 of the GS downstream from its separation from the U.S. continental slope. Boundary conditions
187 are supplied by a sequence of two lower-resolution simulations that span the entire GS region and
188 the Atlantic basin, respectively. The simulation is forced by daily winds and diurnally modulated
189 surface fluxes. The modelling approach is described in detail in Gula et. al²¹.

190 Virtual Lagrangian Particles. The neutrally buoyant Lagrangian (flow-following) particles
191 were seeded at time 285 and advected both backwards and forwards from this time by the model
192 velocity fields without additional dispersion from the model's mixing processes²². A 4th-order
193 Runge-Kutta method with a time step $dt = 1 \text{ s}$ is used to compute particle advection. Velocity and
194 tracer fields are interpolated at the positions of the particles using cubic spline interpolation in both
195 the horizontal and vertical directions. We use hourly outputs from the simulation to get sufficiently
196 frequent and temporally-smooth velocity sampling for accurate parcel advection.

197

- 198 1. Joyce, T. M., Thomas, L. N., Dewar, W. K. & Girton, J. B. Eighteen degree water formation
199 within the Gulf Stream during CLIMODE. *Deep Sea Res. II* (2013).
- 200 2. Johns, W., Shay, T., Bane, J. & Watts, D. Gulf stream structure, transport, and recirculation
201 near 68 w. *J. Geophys. Res.* **100**, 817–817 (1995).
- 202 3. Ford, W., Longard, J. & Banks, R. On the nature, occurrence and origin of cold low salinity
203 water along the edge of the Gulf Stream. *J. Mar. Res.* **11**, 281–293 (1952).
- 204 4. Churchill, J. H., Cornillon, P. C. & Hamilton, P. Velocity and hydrographic structure of sub-
205 surface shelf water at the Gulf Stream’s edge. *J. Geophys. Res.* **94**, 10791–10800 (1989). URL
206 <http://dx.doi.org/10.1029/JC094iC08p10791>.
- 207 5. Rajamony, J., Hebert, D. & Rossby, T. The cross-stream potential vorticity front and its role
208 in meander-induced exchange in the gulf stream. *J. Phys. Oceanogr.* **31**, 3551–3568 (2001).
- 209 6. Marshall, J., Shuckburgh, E., Jones, H. & Hill, C. Estimates and implications of surface
210 eddy diffusivity in the Southern Ocean derived from tracer transport. *J. Phys. Oceanogr.* **36**,
211 1806–1821 (2006).
- 212 7. Naveira Garabato, A. C., Ferrari, R. & Polzin, K. L. Eddy stirring in the southern ocean. *J.*
213 *Geophys. Res.* **116** (2011).
- 214 8. Bower, A. S., Rossby, H. T. & Lillibridge, J. L. The Gulf Stream-barrier or blender? *J. Phys.*
215 *Oceanogr.* **15**, 24–32 (1985).

- 216 9. Bower, A. & Rossby, T. Evidence of cross-frontal exchange processes in the Gulf Stream
- 217 based on isopycnal rafos float data. *J. Phys. Oceanogr.* **19**, 1177–1190 (1989).
- 218 10. Bower, A. S. & Lozier, M. S. A closer look at particle exchange in the Gulf Stream. *J. Phys.*
- 219 *Oceanogr.* **24**, 1399–1418 (1994).
- 220 11. Flierl, G., Malanotte-Rizzoli, P. & Zabusky, N. Nonlinear waves and coherent vortex structures
- 221 in barotropic β -plane jets. *J. Phys. Oceanogr.* **17**, 1408–1438 (1987).
- 222 12. Stern, M. E. Lateral wave breaking and “shingle” formation in large-scale shear flow. *J. Phys.*
- 223 *Oceanogr.* **15**, 1274–1283 (1985).
- 224 13. Pratt, L. J., Susan Lozier, M. & Beliakova, N. Parcel trajectories in quasigeostrophic jets:
- 225 Neutral modes. *J. Phys. Oceanogr.* **25**, 1451–1466 (1995).
- 226 14. Lozier, M., Pratt, L., Rogerson, A. & Miller, P. Exchange geometry revealed by float trajecto-
- 227 ries in the Gulf Stream. *J. Phys. Oceanogr.* **27**, 2327–2341 (1997).
- 228 15. Song, T., Rossby, T. & Carter, E. Lagrangian studies of fluid exchange between the Gulf
- 229 Stream and surrounding waters. *J. Phys. Oceanogr.* **25**, 46–63 (1995).
- 230 16. Bower, A. S. A simple kinematic mechanism for mixing fluid parcels across a meandering jet.
- 231 *J. Phys. Oceanogr.* **21**, 173–180 (1991).
- 232 17. Thomas, L. N. & Shakespeare, C. A new mechanism for mode water formation involving
- 233 cabbeling and frontogenetic strain at thermohaline fronts. In press *J. Phys. Oceanogr.*

- 234 18. Whitt, D. B. & Thomas, L. N. Near-inertial waves in strongly baroclinic currents. *J. Phys.*
235 *Oceanogr.* **43**, 706–725 (2013).
- 236 19. Firing, E., Hummon, J. M. & Chereskin, T. K. Improving the quality and accessibility of
237 current profile measurements in the southern ocean. *Oceanography* (2012).
- 238 20. Shchepetkin, A. & McWilliams, J. The regional oceanic modeling system (ROMS): a split-
239 explicit, free-surface, topography-following-coordinate oceanic model. *Ocean Modell.* **9**, 347–
240 404 (2005).
- 241 21. Gula, J., Molemaker, M. J. & McWilliams, J. C. Gulf stream dynamics along the southeastern
242 us seaboard. *J. Phys. Oceanogr.* **45**, 690–715 (2015).
- 243 22. Gula, J., Molemaker, M. J. & McWilliams, J. C. Submesoscale cold filaments in the gulf
244 stream. *J. Phys. Oceanogr.* **44**, 2617–2643 (2014).

245 List of Figures

256	2 Cross sections of data collected across the Gulf Stream. Y is the cross-stream	
257	distance perpendicular to the path of the float, positive being northwards. The four	
258	columns correspond to the four sections labeled a-d in Fig. 1. Potential density is	
259	contoured in black and $\sigma_\theta = 26.25 \text{ kg m}^{-3}$ is magenta. Along a constant density	
260	surface salty water is warmer than fresher water, so the GS on the left is warm	
261	and salty. Section a) is the furthest upstream section (65W) and d) is the furthest	
262	downstream (63.75 W) (Fig. 3b). e)-h) downstream velocity calculated relative to	
263	the float's trajectory by removing the float's mean speed of $u_{float} = 1.4 \text{ m s}^{-1}$ for	
264	the observation period. Green contours are regions in temperature-salinity space	
265	labeled “streamers” in Fig. 3a. i)-l) Potential vorticity sections (see text);	19
266	3 Streamer properties and distribution in space. a) Logarithmically scaled his-	
267	togram in temperature-salinity space (colours). The warm-salty GS water is very	
268	distinct from the water to the north, which is cold and fresh. The water near the	
269	surface is heavily modified by the atmosphere. Deeper, there is a class of water	
270	distinct from the GS water and the water to the north, that we label “streamers”.	
271	This water is contoured in green in Fig. 2e-l. b) Interpolation of salinity, velocity,	
272	and potential vorticity onto the $\sigma_\theta = 26.25 \text{ kg m}^{-3}$ isopycnal, plotted geographi-	
273	cally (with a small exaggeration of scale in the north-south direction, and the latter	
274	two fields offset slightly to the south-east). This used data from both ships. The	
275	ship track for the <i>Atlantis</i> is plotted in black, and the four cross-sections in Fig. 2	
276	are plotted in magenta. The streamer water is contoured in green.	20

300 **Acknowledgements** Our thanks to the captains and crews of *R/V Knorr* and *R/V Atlantis*, The AVHRR
301 Oceans Pathfinder SST data were obtained from the Physical Oceanography Distributed Active Archive Cen-
302 ter (PO.DAAC) at the NASA Jet Propulsion Laboratory, Pasadena, CA. <http://podaac.jpl.nasa.gov>. Funding
303 was supplied by Office of Naval Research, Grants XXXXXX

304 **Competing Interests** The authors declare that they have no competing financial interests.

305 **Correspondence** Correspondence and requests for materials should be addressed to Jody M. Klymak. (email:
306 jklymak@uvic.ca).

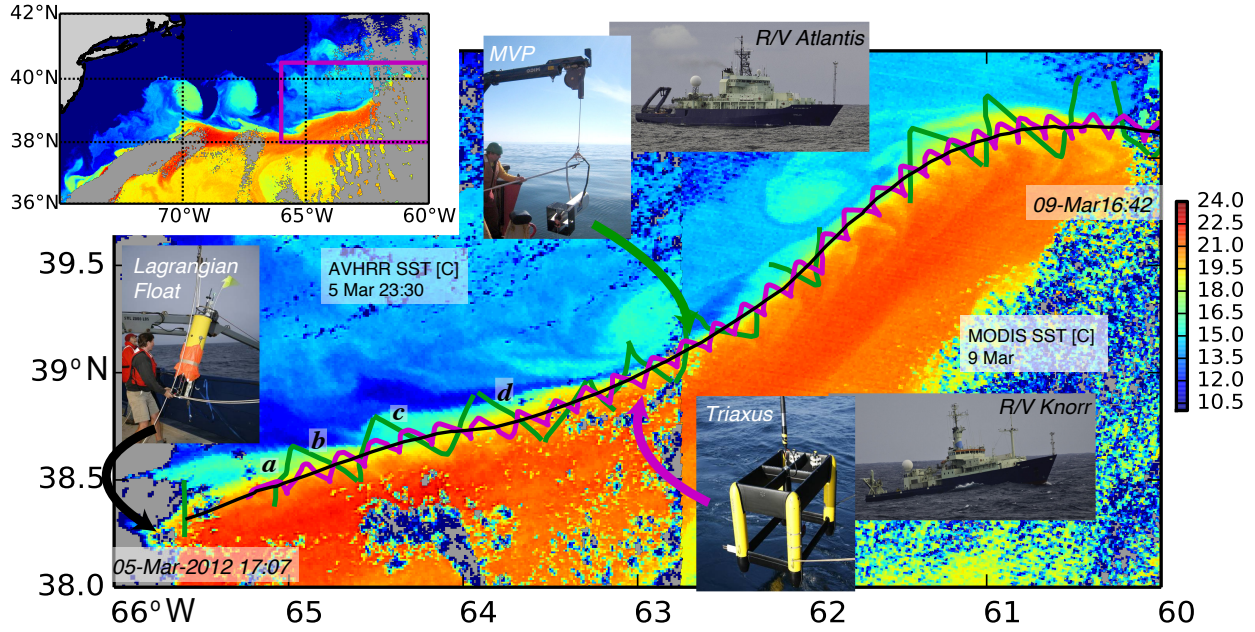


Figure 1: Experimental design. Inset: The experiment site on the north wall of the Gulf Stream, between 66 and 60 W, as shown in an AVHRR satellite image of sea surface temperature (SST). Main: Detailed SST image composed from two satellites images. The GS is warm and delineated by a sharp front. There are small sub-mesoscale structures north of the front, which are the focus of this paper. The satellite images are a composite from early in the observation period (AVHRR 6 Mar), and late (MODIS, 9 Mar). A Lagrangian float was deployed in the front (black curve), and the ship tracks bracketed the float's position (green: *R/V Atlantis*, magenta: *R/V Knorr*). *R/V Atlantis* cross-sections labeled a-d are shown in Fig. 2a-d.

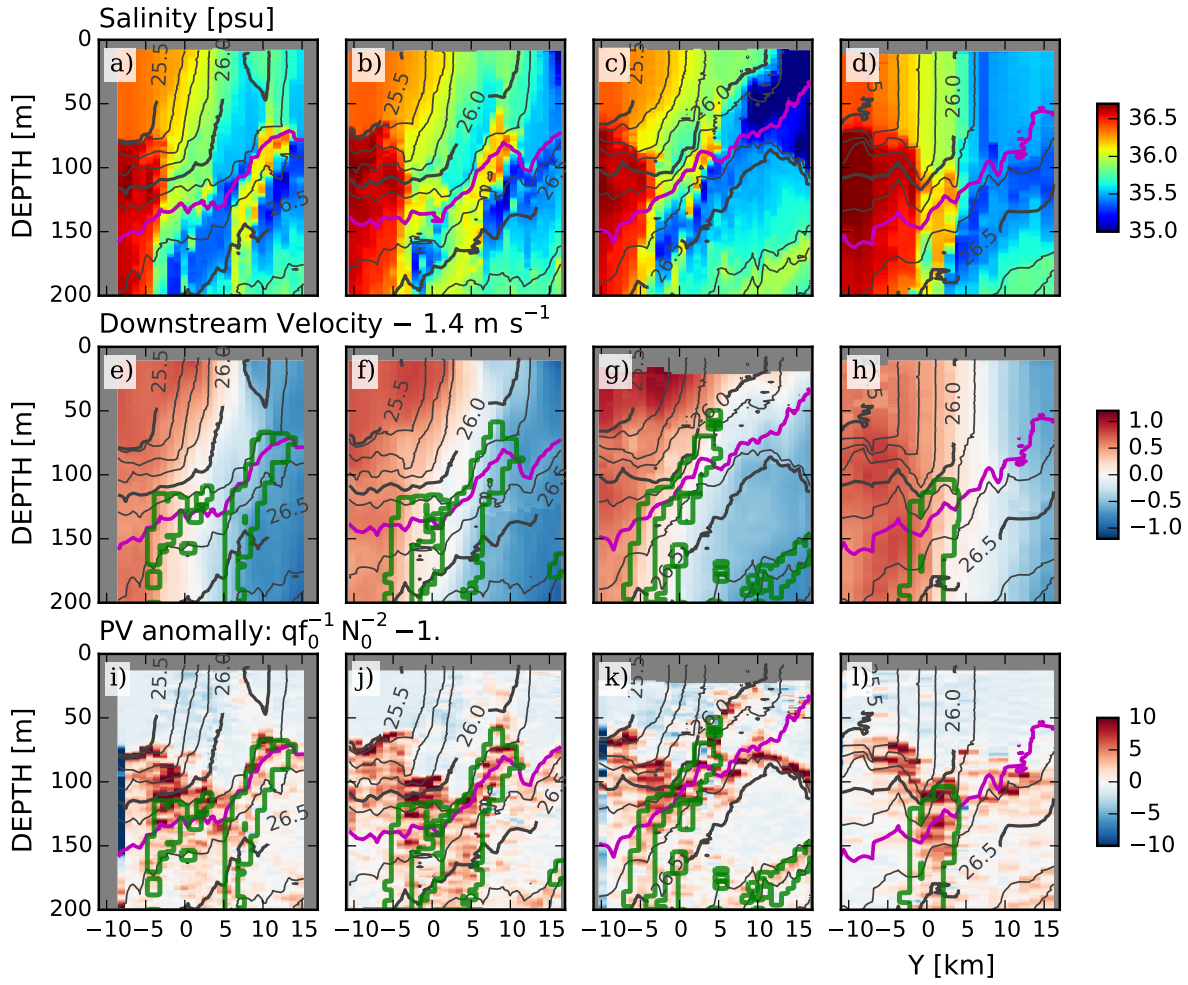


Figure 2: Cross sections of data collected across the Gulf Stream. Y is the cross-stream distance perpendicular to the path of the float, positive being northwards. The four columns correspond to the four sections labeled a-d in Fig. 1. Potential density is contoured in black and $\sigma_\theta = 26.25 \text{ kg m}^{-3}$ is magenta. Along a constant density surface salty water is warmer than fresher water, so the GS on the left is warm and salty. Section a) is the furthest upstream section (65W) and d) is the furthest downstream (63.75 W) (Fig. 3b). e)–h) downstream velocity calculated relative to the float's trajectory by removing the float's mean speed of $u_{\text{float}} = 1.4 \text{ m s}^{-1}$ for the observation period. Green contours are regions in temperature-salinity space labeled “streamers” in Fig. 3a. i)–l) Potential vorticity sections (see text);

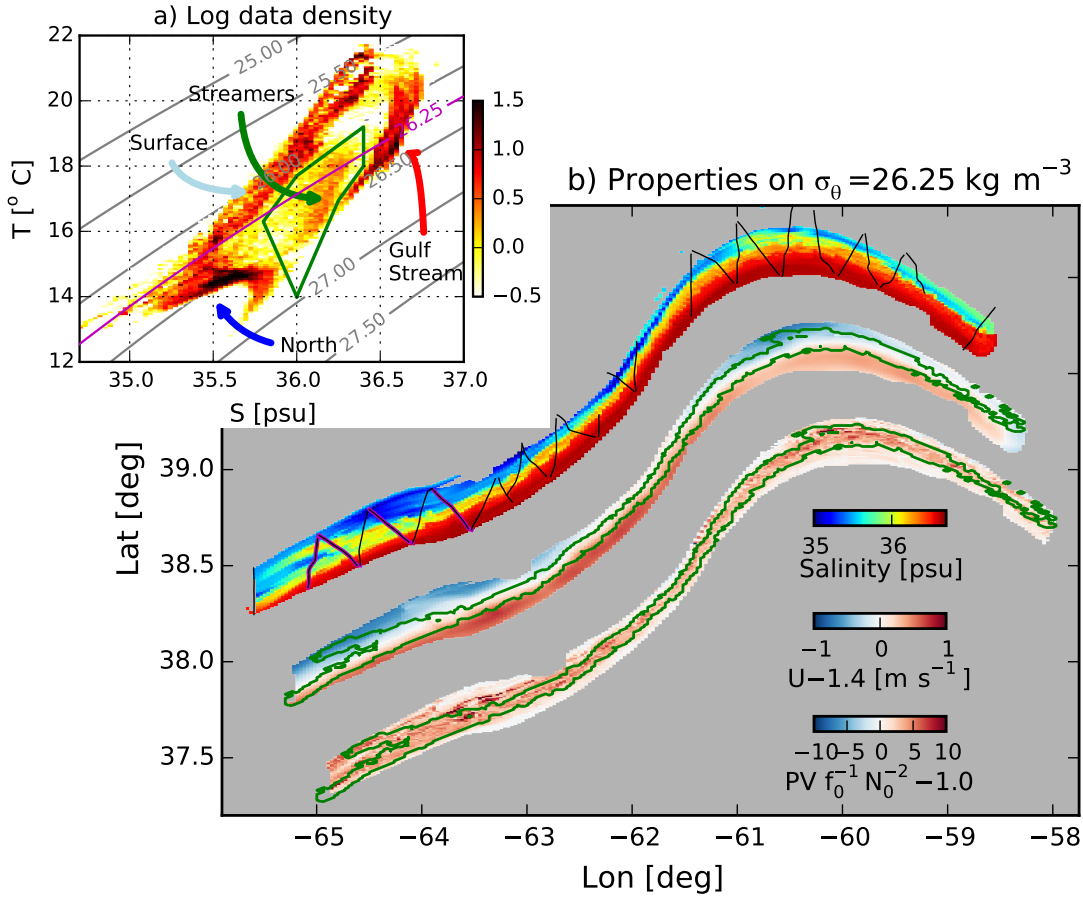


Figure 3: Streamer properties and distribution in space. a) Logarithmically scaled histogram in temperature-salinity space (colours). The warm-salty GS water is very distinct from the water to the north, which is cold and fresh. The water near the surface is heavily modified by the atmosphere. Deeper, there is a class of water distinct from the GS water and the water to the north, that we label “streamers”. This water is contoured in green in Fig. 2e-l. b) Interpolation of salinity, velocity, and potential vorticity onto the $\sigma_\theta = 26.25 \text{ kg m}^{-3}$ isopycnal, plotted geographically (with a small exaggeration of scale in the north-south direction, and the latter two fields offset slightly to the south-east). This used data from both ships. The ship track for the *Atlantis* is plotted in black, and the four cross-sections in Fig. 2 are plotted in magenta. The streamer water is contoured in green.

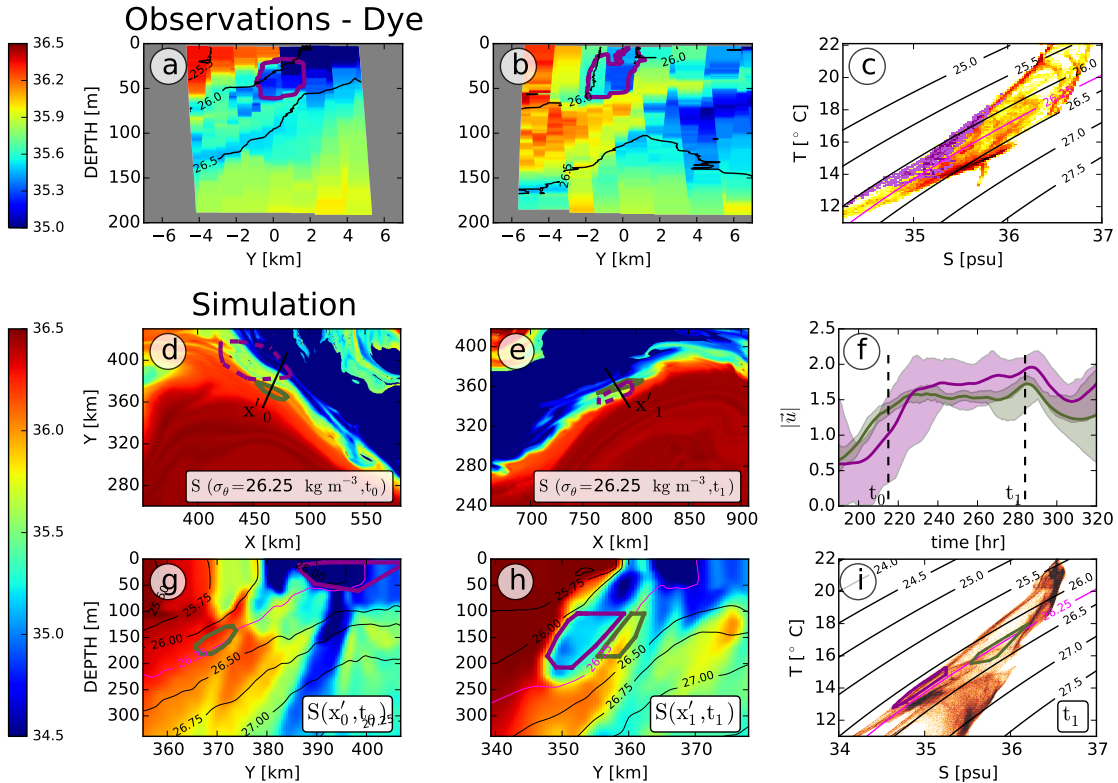


Figure 4: **Evidence for entrainment of intrusions from a dye release and numerical simulation.**

a) Salinity section from an occupation of the GS 14 March. The location of a dye is contoured in magenta. b) Salinity section from downstream. A streamer has enfolded the dye in cold-fresh water between itself and the GS. c) Temperature-salinity diagram for this occupation. The temperature-salinity for the dye is coloured in dark magenta. d) Salinity in the GS on the $\sigma_\theta = 26.25 \text{ kg m}^{-3}$ isopycnal from a high-resolution numerical simulation at t_0 . The green contours delineate the location of particles seeded downstream in the streamer at time $t_1 = t_0 + 70\text{h}$ (see panels e and h) and advected *backwards* in time to t_0 showing where the streamer water originated. The dark magenta contour is the location of particles seeded in the fresh intrusion. The straight line shows the location of the salinity cross-section in panel g. e) as panel d, except at $t_1 = t_0 + 70\text{ h}$; this is the time and locations where the two clouds of particles were seeded. g) and h) salinity cross sections for times t_0 and t_1 . The location of the particles is shown in green and dark magenta contours. The $\sigma_\theta = 26.25 \text{ kg m}^{-3}$ isopycnal is contoured in light magenta. These panels show that the origin of the streamer water was in the GS front, and that the fresh-cold water